Published in final edited form as:
Acta Neuropathol. 2013 June ; 125(6): 879–889. doi:10.1007/s00401-013-1108-7.

Lingo-1 Expression is Increased in Essential Tremor Cerebellum and is Present in the Basket Cell Pinceau

Sheng-Han Kuo, MD[1], **Guomei Tang, PhD**[1], **Elan D. Louis, MD MSc**[1,2,3,4], **Karen Ma, MS**[3], **Rachel Babij, MS**[3], **Matthew Balatbat, MS**[3], **Etty Cortes, MD**[2,5], **Jean-Paul G. Vonsattel, MD**[2,5], **Ai Yamamoto, PhD**[1,5], **David Sulzer, PhD**[1], and **Phyllis L. Faust, MD PhD**[5]

[1]Department of Neurology, College of Physicians and Surgeons, Columbia University, New York, NY, USA

[2]Taub Institute for Research on Alzheimer's Disease and the Aging Brain, College of Physicians and Surgeons, Columbia University, New York, NY, USA

[3]GH Sergievsky Center, College of Physicians and Surgeons, Columbia University, New York, NY, USA

[4]Department of Epidemiology, Mailman School of Public Health, Columbia University, New York, NY, USA

[5]Department of Pathology and Cell Biology, Columbia University Medical Center and the New York Presbyterian Hospital, New York, NY, USA

Abstract

The Lingo-1 sequence variant has been associated with essential tremor (ET) in several genome wide association studies. However, the role that Lingo-1 might play in pathogenesis of ET is not understood. Since Lingo-1 protein is a negative regulator of axonal regeneration and neurite outgrowth, it could contribute to Purkinje cell (PC) or basket cell axonal pathology observed in postmortem studies of ET brains. In this study, we used Western blotting and immunohistochemistry to examine Lingo-1 protein in ET vs. control brains. In Western blots, Lingo-1 protein expression level was significantly increased in cerebellar cortex (1.56 ± 0.46 in ET cases vs. 0.99 ± 0.20 in controls, $p = 0.002$), but was similar in the occipital cortex ($p = 1.00$) of ET cases vs. controls. Lingo-1 immunohistochemistry in cerebellum revealed that Lingo-1 was enriched in the distal axonal processes of basket cells, which formed a "pinceau" structure around the PC axon initial segment (AIS). We found that some Lingo-1 positive pinceau had abnormally elongated processes, targeting PC axon segments distal to the AIS. In ET cases, the percentage of Lingo-1 positive pinceau that were ≥30μm or ≥40 μm in length was increased 2.4- to 4.1-fold, respectively, vs. pinceau seen in control brains ($p<0.0001$). Elongated Lingo-1 positive pinceau strongly correlated with number of PC axonal torpedoes and a rating of basket cell axonal pathology. The increased cerebellar Lingo-1 expression and elongated Lingo-1 positive pinceau processes could contribute to the abnormal PC and basket cell axonal pathology and cerebellar dysfunction observed in ET.

Correspondence: Dr. Sheng-Han Kuo, 710 West 168th Street, 3rd floor, New York, NY 10032, USA, Tel: (212)305-5558, Fax: (212)305-1304, sk3295@columbia.edu.

Statistical Analyses: The statistical analyses were conducted by Drs. Kuo and Louis.

Disclosure: The authors report no conflicts of interest.

Keywords

Essential tremor; pathology; cerebellum; basket cells; Lingo-1

Introduction

Essential tremor (ET) is among the most common movement disorders, with a prevalence of more than 4% over the age of 65 [25]. Many ET patients have a family history of ET, which seems to follow an autosomal dominant pattern of transmission [43]. Several studies identified Lingo-1 polymorphisms as a risk factor for ET [9, 42, 44, 45, 48, 49]; however, how Lingo-1 confers an increased risk of ET remains poorly understood.

In several neuroimaging studies in ET, the cerebellum has been consistently identified as an affected brain region [11]. In addition, strokes disrupting cortico-cerebellar pathways can lessen tremor in ET patients, supporting the role of cerebellum in tremor generation [12]. Recent postmortem studies have identified an increasing number of structural and degenerative changes in ET cerebellum relative to age-matched control brains, including a 6–7 fold increase in Purkinje cell (PC) axonal swellings (i.e., torpedoes), significant PC loss (approximately 30 – 40%) in some studies, heterotopic PCs, and an increase in Bergmann gliosis [2, 19, 24, 39]. In addition, basket cell axonal processes surrounding the PC soma in ET brains often have a dense and tangled appearance, indicating that structural alterations in other neurons within the PC functional network may also contribute to ET pathogenesis [13]. On the other hand, parallel fibers seem to be relatively unaffected in ET [20]. In addition to cerebellar cortical changes, more extensive degenerative changes within the deep cerebellar nuclei has been observed in some ET cases, [27] and loss of *gamma*-aminobutyric acid $(GABA)_A$ and $GABA_B$ receptors in the dentate nucleus has also been described in ET [36]. While these cerebellar structural changes support a central role of the cerebellum in ET, the precise mechanisms whereby these changes lead to a tremor phenotype remain poorly understood.

Lingo-1 is selectively expressed in the central nervous system and is widely distributed in different brain regions including the cerebellum, inferior olivary nucleus, substantia nigra, and cerebral cortex [3, 18, 21]. Within these regions, Lingo-1 is enriched in neurons and oligodendrocytes [32]. Lingo-1 forms a ternary complex with Nogo-66 receptor (NgR1) and p75 neurotrophin receptor ($p75^{NTR}$) or TROY to form a NgR1 complex [32, 38]. NgR1 complex binds to inhibitory molecules such as Nogo-A, which then activates RhoA as a negative regulator for neurite outgrowth [22, 29, 32, 51]. Inhibition of Lingo-1 promotes dopaminergic neurite outgrowth and neuronal protection in the MPP+ toxin model of Parkinson disease (PD) [18] and enhances oligodendrocyte maturation [30,31]. In the cerebellum, Nogo-A mediated neurite-myelin interactions regulates axonal sprouting in PCs, preventing aberrant growth of PC axons and stabilizing intracortical connectivity [14].

Since the Lingo-1 protein is a negative regulator of axonal regeneration and neurite outgrowth, it could contribute to the PC or basket cell axonal pathology observed in postmortem studies of ET brains. In this study, we determined the expression level and cellular distribution of Lingo-1 protein in the cerebellar cortex of ET cases vs. controls.

Methods

Brain Repository and Study Subjects

The study was conducted at the Essential Tremor Centralized Brain Repository (ETCBR), New York Brain Bank (NYBB), Columbia University, New York. Postmortem tissue was

obtained from ET cases and age-matched non-diseased controls with a comprehensive neuropathological diagnostic assessment as previously described [47].

The clinical diagnosis of ET was initially assigned by treating neurologists, and then confirmed by an ETCBR study neurologist using medical records, a detailed, videotaped, neurological assessment, and ETCBR diagnostic criteria [23]. All the ET cases and controls are Caucasians and none of them have a history of traumatic brain injury or heavy ethanol use, as previously defined [17]. Non-diseased control brains were obtained from the NYBB, and were from individuals followed at the Alzheimer disease (AD) Research Center or the Washington Heights Inwood Columbia Aging Project at Columbia University. They were followed prospectively with serial neurological examinations and were clinically free of AD, ET, PD, Lewy body dementia, or progressive supranuclear palsy. All brains received ratings of neurofibrillary tangles using Braak and Braak staging [5, 6], and Consortium to Establish a Registry for AD (CERAD) ratings for neuritic plaques [33]. Other neuropathological changes are detailed in Supplemental Table 1. Postmortem interval (PMI) was the number of hours between death and placement of the brain in a cold room or on ice. We selected the available age-matched, non-diseased control brains from NYBB based on age at death to perform immunohistochemistry (IHC) on cerebellar cortical tissue (11 ET cases, 12 controls) and Western blot analyses from cerebellar cortex (10 ET cases, 11 controls) and occipital cortex (7 ET cases, 9 controls. Among these, 6 ET cases and 9 controls were the same cases used for Western blot analysis of the cerebellar cortex).

A standard 3 × 20 × 25 mm parasagittal neocerebellar block was obtained from a 0.3 cm thick parasagittal slice located 1 cm from the cerebellar midline. Paraffin sections (7μm thick) were stained with Luxol Fast Blue Hematoxylin and Eosin (LH&E) or Bielschowsky silver stain as described previously [2, 24]. Axonal torpedoes were quantified in the entire LH&E-stained section. We previously developed a semi-quantitative rating scale to assess basket cell axonal plexus morphology, a basket cell plexus (BP) score (range = 0 – 3), and have shown that a high basket plexus score robustly correlates with number of torpedoes [13]. All clinical demographics and pathological details of the ET cases and controls are shown in Table 1 and Supplemental Table 1. None of the ET or control brains used for cerebellar IHC had any Lewy body pathology. Axonal torpedo counts of 4 of these ET cases and 4 controls were reported previously [24].

In a secondary analysis, we performed Lingo-1 IHC in 9 cases of cerebellar degenerative disorders (Cbl-D) from the NYBB. This included 8 brains of pathologically confirmed multiple system atrophy (MSA), which all had prominent cerebellar degeneration. One additional brain had a genetically confirmed diagnosis of spinocerebellar ataxia type 7. The MSA cases fulfilled the pathological diagnostic criteria of olivopontocerebellar atrophy [46]. For MSA cases, the mean age at death was 66.7 ± 6.1 years, mean brain weight was 1219 ± 81 grams, mean PMI was 8.1 ± 2.0 hours, and 62.5% (5 of 8) were of female gender. For the SCA7 brain, age at death was 39 years, brain weight was 860 grams, and gender was female.

Cerebellar Immunohistochemistry

Cerebellar sections were incubated with polyclonal rabbit anti-Lingo-1 antibody (Millipore, 07-678, 1:100) at 4°C for 48 hours after antigen retrieval in Trilogy (Cell Marque) in a vegetable steamer for 40 minutes, 100°C. The sections were subsequently incubated with goat anti-rabbit IgG horseradish peroxidase conjugated antibody (Jackson ImmunoResearch 1:100), followed by 3,3'-diaminobenzidine (DAB) precipitation. This Lingo-1 antibody was previously used in a study on paraffin-embedded human multiple sclerosis (MS) brain tissue [37]. This Lingo-1 antibody (Millipore) and another Lingo-1 antibody (Abcam ab23631) both recognize the same band in Western blots from human frozen brain samples (see below, Western blot analysis). We also tested the immunohistochemical specificity of this

Lingo-1 antibody with Lingo-1 peptide blockade (Abcam, ab25890) (Supplemental Figure 1); this peptide is within the c-terminal 20 amino acids of human Lingo-1 used as immunogen. Lingo-1 peptide and Lingo-1 antibody at 10:1 molar ratio or Lingo-1 antibody alone were incubated at 4°C for 24 hours and were then used as the primary antibody for IHC.

Immunofluorescence studies were performed with antibodies to Lingo-1 and secondary Alexa 488 donkey anti-rabbit IgG antibody (Invitrogen, 1:100). For dual localization studies, Lingo-1 antibodies (1:100) were co-incubated with mouse monoclonal antibodies to glial fibrillary acidic protein (GFAP) (Sigma 1:100), myelin basic protein (MBP) (SMI99, Covance 1:100), CD68 (DAKO 1:100), phosphorylated-neurofilament (SMI31, Covance 1:100), glutamatic acid decarboxylase (GAD) (MBL International, 1:100), or parvalbumin (Swant, #235, 1:100). The secondary antibodies were anti-rabbit IgG or anti-mouse IgG conjugated with Alexa fluorophore 488 or 594 (1:100). Microscopic images were obtained by confocal microscopy (Leica) or bright field microscopy (Olympus).

Morphologic features of the Lingo-1 immunopositive plexus around proximal PC axons were quantified in the DAB-light microscopic cerebellar sections. All morphological measurements were done by a rater blinded to the diagnosis, with a piece of colored tape coded with an English alphabet character covering the identification number on each slide, and random ordering of cases versus control specimens within the alphabetic blinded code. A neuropathologist (PLF) randomly selected 20 fields in the cerebellar cortex with a 20X objective lens and quantified the percentage of PC bodies associated with Lingo-1 immunopositive structures and the mean number of Lingo-1 immunopositive structures per 200× microscopic field. The area occupied by Lingo-1 pinceau in each brain was analyzed in Image J software from digital images of 15–20 randomly selected microscopic fields with 40X objective lens. The length of the Lingo-1 immunopositive plexus around the PC axon initial segment (AIS) was measured with an eyepiece micrometer using a 40X objective lens, extending from the apex of the pinceau at the base of the PC body to the distal most process along the adjacent PC axon. Plexus length was measured on at least 100 consecutive plexuses within each immunostained section, and the percent of Lingo-1 plexuses with length ≥30μm, ≥40 or ≥50 μm was determined. The diagnosis was unblinded at the data analysis stage.

Western Blot Analysis

Frozen cerebellar cortex (10 ET, 11 controls) or occipital cortex (7 ET, 9 controls) in standardized vials was solubilized in RIPA buffer (Sigma) with proteinase inhibitors (Roche Diagnostics) and phosphatase inhibitors (Sigma) and was sonicated followed by centrifugation at 16,870 g for 30 minutes. Proteins (20μg; Bradford assay) were separated on a NuPAGE Novex 4–12% Gel (Invitrogen) and transferred to a nitrocellulose membrane (Bio-Rad). Blots were incubated with primary antibodies to Lingo-1 (Abcam ab23631 1:1000) and β-actin (1:1000, Sigma) followed by horseradish peroxidase-conjugated anti-mouse or anti-rabbit secondary antibodies (Thermo scientific, 1:10,000). Signals were detected with ECL (Millipore) and Kodak BioMax MR films (Sigma). Films were analyzed with ImageQuant (Amersham Biosciences, Piscataway, NJ) by a rater blinded to the diagnosis. The Lingo-1 signal was normalized to β-actin for each sample. Each Western blot was repeated three times to obtain an average value in each sample, expressed as relative to the average control value, arbitrarily set at 1.0.

Data Analyses

Analyses were performed in GraphPad Prism (v 5.0). Demographic and clinical characteristics of ET cases and controls were compared using Student's t tests and chi

square tests. The percentage of PC bodies associated with Lingo-1 positive PC AIS plexuses, the total number of Lingo-1 labeled PC plexuses in a given 200X microscopic field, the length of the Lingo-1 immunopositive PC plexus, and the Lingo-1 protein level in the cerebellum all followed a normal statistical distribution (Kolmogorov–Smirnov test). We used a parametric test (Student's t test) to assess all IHC and Western blot results. We used ANOVA analysis to compare the percentage of the Lingo-1 immunopositive plexus ≥30 μm, ≥40 μm, or ≥50 μm in ET cases, Cbl-D cases, and controls and Tukey's post hoc test.

Results

Increased Lingo-1 protein expression in cerebellum of ET brains

We used Western blot analysis to determine the Lingo-1 protein levels in the cerebellar cortex of 10 ET cases and 11 controls (Figure 1). The mean Lingo-1 protein level was nearly 60% higher in ET cases than controls (1.56 ± 0.46 vs. 0.99 ± 0.20, p = 0.002) (Figure 1a, b). Two ET cases had incidental Lewy bodies (Table 1); even if these two samples were excluded from this analysis, the mean Lingo-1 protein level was still significantly elevated (1.46 ± 0.44, p = 0.02). We next analyzed Lingo-1 protein levels in the occipital cortex of 7 ET cases and 9 controls to determine whether the increased Lingo-1 level was specific to the cerebellum. The Lingo-1 level in the ET occipital cortex did not follow a normal statistical distribution (Kolmogorov–Smirnov test, $p<0.02$) due to the presence of one outlier that was 5 SDs above the mean of the remaining samples; excluding the outlier made the distribution normal (Kolmogorov–Smirnov test, $p>0.10$). Excluding the outlier, ET cases had similar Lingo-1 levels in occipital cortex compared to the controls (1.07 ± 0.21 in ET cases vs. 1.00 ± 0.22 in controls, $p = 1.00$)(Figure 1c, d). Including the one outlier also produced similar results (1.22 ± 0.44 in ET cases vs. 1.00 ± 0.22 in controls, $p = 0.61$). In the cerebellum, Lingo-1 protein level was not significantly correlated with torpedo counts ($r = 0.15$, $p = 0.54$) and BP morphology rating (BP score) ($r = 0.17$, $p = 0.48$).

Lingo-1 is associated with a PC AIS plexus

We performed IHC to assess the cell type specificity of Lingo-1 expression in the cerebellum. We found that the Lingo-1 expression was highly enriched in a plexus of thin processes surrounding the PC AIS (Figure 2a, arrows), which often formed a distinct cone shape extending along the PC AIS in the granule cell layer (Figure 2b). The morphology of this plexus was highly similar to the "pinceau" structure produced by distal processes of basket interneurons in cerebellar cortex [35]. These Lingo-1 stained processes often had distinct small swellings, suggestive of synaptic structures (Figure 2b, c). Lingo-1 stained processes were predominantly localized around the PC AIS, but occasionally extended to more distal segments of PC axons (Figure 2d, e). Interestingly, Lingo-1 fibers surrounded the PC axon proximal to torpedoes (Figure 2f, i), and only very rarely were observed adjacent to the torpedo itself (data not shown). The Lingo-1 plexus was occasionally seen to form a complex linear extension between adjacent PCs (Figure 2g, h). The Lingo-1 plexus was observed adjacent to, but not consistently colocalizing with, PC recurrent collateral processes (Figure 2j,k, large arrowheads), suggesting that these Lingo-1 processes are not innervating PC recurrent collaterals. Lingo-1 immunostains also showed weaker labeling along axonal profiles in subcortical white matter and fainter labeling of PC bodies and the cerebellar molecular layer (Figure 2a). Lingo-1 peptide reliably and robustly blocked the staining of the plexus surrounding the PC AIS and staining of PC bodies and molecular layer, and partially blocked the staining in the cerebellar subcortical white matter (Supplemental Figure 1).

We further investigated the cell types expressing Lingo-1 in the AIS plexus, using dual-immunofluorescence staining to colocalize Lingo-1 with markers for glial or axonal

processes in brain. However, Lingo-1 plexus did not colocalize with astrocyte marker, GFAP (Figure 3a–c), oligodendrocyte myelin marker, MBP (Figure 3d–f), axonal marker, phosphorylated neurofilament (Figure 3g–i) or macrophage marker, CD68 (data not shown).

The absence of neurofilament colocalization does not exclude the possibility that these Lingo-1-labeled processes represent distal axonal-synaptic structures, as axon terminals, and in particular the basket cell pinceau, are not enriched with neurofilaments [41]. Indeed, these Lingo-1 structures strongly co-localized with the neuronal synaptic marker synaptophysin, indicating that they contain pre-synaptic processes (Figure 4a–f). Cerebellar sections immunostained with both Lingo-1 and GAD antibodies show colocalization in synapses around the PC AIS (Figure 4g–l), consistent with GABA containing pinceau synapses [1]. While GAD and neurofilament antibodies also label basket cell axonal processes that surround PC soma, the perisomal basket processes were not strongly labeled with Lingo-1 antibody (Figure 4g–l; Figure 2b, g–h), indicating that these Lingo-1-labeled processes represent basket cell distal axons associated with PC AIS. Lingo-1 also colocalizes with parvalbumin labeling of the basket cell pinceau (Figure 4m–o), as well as GAD positive basket cell axonal plexus connecting two adjacent PCs (Figure 4p–r).

Elongated Lingo-1 positive pinceau morphology in ET brains

We quantified several morphologic features of the Lingo-1 pinceau plexus around proximal PC axons in ET vs. control brains (Figure 5). The percentage of PCs in each brain section that contained a Lingo-1 labeled plexus was similar in ET cases and controls (41.4 ± 16.0% in ET cases vs. 39.5 ± 24.5% in controls, $p = 0.77$) (Figure 5a). The Lingo-1 labeled plexus was also seen in the absence of a PC body (Figure 2a), which may be a sectioning artifact or similar to “empty baskets” as seen in Bielschowsky silver stained sections [13]. However, the mean number of total Lingo-1 labeled plexuses per 20X microscopic field was also similar in ET cases and controls (3.7 ± 1.5 in ET cases vs. 3.9 ± 2.7 in controls, $p = 0.22$) (Figure 5b). Lastly, the area occupied by the Lingo-1 plexus, measured with Image J software, was also highly similar in ET cases and controls (293.4 ± 43.1 μm^2 in ET cases vs. 283.8 ± 31.5 μm^2 in controls, $p=0.85$) (Supplemental Figure 2). These findings indicate that the Lingo-1 axonal plexus labeling represents a normal structure in cerebellar cortex, which is morphologically and immunohistochemically consistent with the basket cell pinceau.

In a paraffin section, the Lingo-1 labeled pinceau is often seen as a very short segment (Figure 5c1, arrowheads) or, when more fully visualized, a cone-shaped structure (Figure 5c1, black arrows), which all measure a length of 20–25 μm or less along the PC AIS (e.g., 90.8 ± 3.7% of labeled pinceau in controls and 81.2 ± 4.9% in ET cases are ≤25 μm). A ≤25 μm length for many basket cell pinceau is similar to the measured length of ~17–20 μm for the PC AIS [40, 41]. However, we also identified Lingo-1 labeled pinceau processes extending to more distal parts of the PC axon, measuring as long as 30–100 μm from the base of the PC body (Figure 5c1-c5; Figure 2e). Elongated Lingo-1 labeled pinceau measuring ≥30 μm, ≥40 μm, or ≥50 μm in length were 2.4-fold, 4.1-fold or 4.4-fold, respectively, more frequently seen in ET *vs.* control brains (Figure 5d, e, f; for percentage ≥30 μm, 15.9% ± 4.1% in ET cases vs. 6.6% ± 3.2% in controls, $p<0.0001$; for percentage ≥40μm, 6.5% ± 2.1% in ET cases vs. 1.6% ± 1.3% in controls, $p<0.0001$; for percentage ≥50μm, 3.1% ± 1.3% in ET cases vs. 0.7% ± 0.7% in controls, $p<0.0001$). The percentage of elongated Lingo-1 pinceau was strongly correlated with the number of torpedoes (for percentage ≥30 μm, Pearson’s correlation coefficient [r] =0.606, $p=0.008$; for percentage ≥40 μm, $r=0.590$, $p=0.010$; for percentage ≥50 μm, $r=0.474$, $p=0.0006$) and the BP score (for percentage ≥30 μm, $r=0.474$, $p=0.025$; for percentage ≥40 μm, $r=0.491$, $p=0.038$; for percentage ≥50 μm, $r=0.264$, $p=0.029$). Thus, Lingo-1 IHC identifies a novel morphologic alteration in the basket cell pinceau, which correlates with measures of PC and basket cell pathology that are more commonly seen in ET brains.

As a secondary analysis, we performed Lingo-1 IHC and measured the pinceau length in brains with Cbl-D, including MSA (n=8) and SCA7 (n=1), as proximal changes in PC axons are a frequent finding along with profound PC loss. The percentage of Lingo-1 pinceau with length ≥30 μm was significantly increased 2.1-fold in Cbl-D *vs.* control brains ($p<0.0001$), to an extent similar to that seen in ET brains (15.9% ± 4.1% in ET cases vs. 14.1% ± 2.7% in Cbl-D, $p=0.46$) (Figure 5d). However, while Lingo-1 pinceau with length ≥40 μm were still increased 2.2-fold in Cbl-D *vs.* control brains ($p=0.017$), they were significantly less frequently seen than in ET brains (3.7% ± 1.4% in Cbl-D *vs.* 6.5% ± 2.1% in ET cases, $p=0.0014$) (Figure 5e). Very long Lingo-1 pinceau ≥50μm in length were not significantly increased in Cbl-D *vs.* control brains (1.1% ± 0.4% in Cbl-D cases vs. 0.7% ± 0.7% in controls, $p=0.45$), but remained a distinctive feature of the pinceau in ET brains (Figure 5f).

Discussion

Lingo-1 genetic polymorphisms have been identified as a risk factor for ET in a genome wide association study and several follow up studies [9, 42, 44, 45, 48,49]. In this study, we demonstrate that Lingo-1 protein is regionally enriched in the ET cerebellum. At a cellular level, Lingo-1 is highly enriched in a plexus of GAD-positive processes around the PC AIS, consistent with the distal processes of basket cells that form a pinceau [1]. Furthermore, Lingo-1 labeled pinceau processes that target more distal segments of the PC axon are more commonly seen in ET cerebellum than in control brains, and the number of these 'elongated' pinceau correlates with torpedoes and basket cell pathology, providing a novel pathological link between Lingo-1 and ET. Our study raises the possibility that elongated pinceau morphology reflects an underlying degeneration of the PC AIS and/or its adjacent axon, with a disturbance to neuronal polarity that may be a common component of many diseases and injuries that affect the nervous system.

In the current study, we discovered that Lingo-1 is strongly expressed in pinceau processes around the PC AIS, but not in perisomal basket cell processes. The PC AIS is a 10 – 20 μm long segment of unmyelinated axon extending from the axon hillock; it is highly enriched in voltage-gated Na+ channels, cell adhesion molecules (e.g., neurofascin), and cytoskeletal scaffolds (e.g., ankyrin-spectrin-actin), and is critical for initiation of action potentials in PCs and maintenance of neuronal polarity [8, 15, 34, 40]. The pinceau provides GABAergic inhibitory input at the AIS to modulate PC output, although its mechanism of action is unusual as only a few pinceau terminals form axo-axonal synapses with the PC AIS, and the majority of terminals end freely, where they may join other basket cell axons by septate-like junctions or contact glial processes that completely envelop the PC AIS [35]. Several proteins have been reported to cluster specifically in the pinceau, including a number of voltage-activated potassium channel subunits (K_v) and the hyperpolarization-activated and cyclic nucleotide-gated (HCN) channel-1 in basket cell axons [4, 10, 28], and the water channel aquaporin-4 in astrocytic processes of the pinceau [4]. Interestingly, mutations in *Kcna2*, encoding the basket cell pinceau-specific $K_v1.2$, cause defective basket cell inhibitory input to PCs associated with chronic motor-incoordination [50]. The role of Lingo-1 in the function of the pinceau deserves further study.

We did not observe changes in the percentage of PCs associated with Lingo-1 labeled pinceau, or in their density, suggesting that changes in the number of pinceau do not occur in ET cases. Rather, ET cases had significantly increased percentage of Lingo-1 labeled pinceau with elongated processes extending beyond the typically short PC AIS segment, for as long as 30–100 μm from the PC soma. Recent studies in mouse models have demonstrated that a loss of ankyrin G in PCs, or neurofascin in basket cells and/or PCs leads to disorganization of AIS structure and morphologic alterations in the pinceau, including

targeting of basket axons to more distal PC axon segments [1, 7, 52]. Thus, these 'elongated' pinceau processes may be a marker for an underlying alteration in AIS structure.

We also compared the Lingo-1 pinceau length in ET cases and Cbl-D brains. Interestingly, Cbl-D brains have a similar percentage of mildly elongated Lingo-1 pinceau (≥30 μm), but ET cases have a much higher percentage of the moderate to extremely long Lingo-1 pinceau (≥40 μm or ≥50 μm) than seen in Cbl-D and controls. These results demonstrate that elongated Lingo-1 pinceau are a shared feature of cerebellar degeneration in both ET and Cbl-D brains, but they are more frequently longer in ET brains and the extremely long Lingo-1 pinceau is distinctive and relatively specific to ET cases at postmortem examination. It is certainly possible that longer pinceau were more frequently seen in Cbl-D brains at an earlier disease stage, and subsequently degenerated in these end-stage autopsy brains. Nonetheless, our study identifies a novel association of pinceau morphologic alteration and cerebellar cortical degenerations, and the evolution of this change during disease course may lead to further insights into mechanisms of PC degenerations.

We have also demonstrated altered neurofilament distribution in ET PCs that suggest disturbance in the AIS and neuronal polarity, with accumulation of nonphosphorylated neurofilaments in the PC AIS [26], and phosphorylated neurofilaments in PC soma [13]. Interestingly, the size and position of the AIS is also dynamically regulated by electrical activity [16]. Thus, our study demonstrates that basket cell processes may also be remodeled along the PC AIS in ET, which along with PC axonal pathology, contributes to cerebellar dysfunction in ET. The basket cell pinceau provides strong inhibitory input to PCs and modulates the frequency of PC action potential spikes at the AIS, but the means by which morphologic alterations in the pinceau and/or the underlying AIS may lead to tremor generation remains to be investigated.

By Western blot analysis, the expression of Lingo-1 was significantly increased in ET cerebellum, but not in occipital cortex, suggesting that a regionally increased expression of Lingo-1 could contribute to cerebellar dysfunction in ET. Whether this increased Lingo-1 protein expression is specifically associated with the pinceau in ET cases cannot be determined from this study, as cerebellar white matter, PC bodies and molecular layer also have immunohistochemical expression of Lingo-1, although the staining was much lower and less concentrated than in the pinceau (Figure 2a). The role of Lingo-1 in the various cell types and compartments within cerebellum deserves further study.

Our report is the first study to demonstrate that Lingo-1 is regionally increased in ET cerebellum and is enriched at the basket cell pinceau along the PC AIS. Further characterization is needed to elucidate the role of Lingo-1 in regulating PC function and axonal morphology, and evaluating expression of interacting proteins NgR1, TROY, $p75^{NTR}$, in ET cerebellum. Future studies on Lingo-1 expression in other brain regions within cerebellar system pathways, such as inferior olivary nucleus and thalamus, may provide further insight into ET pathogenesis. The extent to which elongated pinceau processes are seen in cerebellum, and possible alterations in the underlying organization of the PC AIS and disturbance to neuronal polarity, remains to be further defined in aging and neurodegenerative diseases.

Supplementary Material

Refer to Web version on PubMed Central for supplementary material.

Acknowledgments

Funding: R01 NS42859 from the National Institutes of Health (Bethesda, MD), Parkinson Disease Foundation, and American Academy of Neurology Clinical Research Training Fellowship.

References

1. Ango F, di Cristo G, Higashiyama H, Bennett V, Wu P, Huang ZJ. Ankyrinbased subcellular gradient of neurofascin, an immunoglobulin family protein, directs GABAergic innervation at purkinje axon initial segment. Cell. 2004; 119:257–272. [PubMed: 15479642]
2. Axelrad JE, Louis ED, Honig LS, et al. Reduced Purkinje cell number in essential tremor: a postmortem study. Arch Neurol. 2008; 65:101–107. [PubMed: 18195146]
3. Barrette B, Vallieres N, Dube M, Lacroix S. Expression profile of receptors for myelin-associated inhibitors of axonal regeneration in the intact and injured mouse central nervous system. Mol Cell Neurosci. 2007; 34:519–538. [PubMed: 17234430]
4. Bobik M, Ellisman MH, Rudy B, Martone ME. Potassium channel subunit Kv3.2 and the water channel aquaporin-4 are selectively localized to cerebellar pinceau. Brain Res. 2004; 1026:168–178. [PubMed: 15488478]
5. Braak H, Alafuzoff I, Arzberger T, Kretzschmar H, Del Tredici K. Staging of Alzheimer disease-associated neurofibrillary pathology using paraffin sections and immunocytochemistry. Acta Neuropathol. 2006; 112:389–404. [PubMed: 16906426]
6. Braak H, Braak E. Diagnostic criteria for neuropathologic assessment of Alzheimer's disease. Neurobiol Aging. 1997; 18:S85–S88. [PubMed: 9330992]
7. Buttermore ED, Piochon C, Wallace ML, Philpot BD, Hansel C, Bhat MA. Pinceau organization in the cerebellum requires distinct functions of neurofascin in Purkinje and basket neurons during postnatal development. J Neurosci. 2012; 32:4724–4742. [PubMed: 22492029]
8. Clark BA, Monsivais P, Branco T, London M, Hausser M. The site of action potential initiation in cerebellar Purkinje neurons. Nat Neurosci. 2005; 8:137–139. [PubMed: 15665877]
9. Clark LN, Park N, Kisselev S, Rios E, Lee JH, Louis ED. Replication of the LINGO1 gene association with essential tremor in a North American population. Eur J Hum Genet. 2010; 18:838–843. [PubMed: 20372186]
10. Chung YH, Shin C, Kim MJ, Lee BK, Cha CI. Immunohistochemical study on the distribution of six members of the Kv1 channel subunits in the rat cerebellum. Brain Res. 2001; 895:173–177. [PubMed: 11259775]
11. Draganski B, Bhatia KP. Brain structure in movement disorders: a neuroimaging perspective. Curr Opin Neurol. 2010; 23:413–419. [PubMed: 20610992]
12. Dupuis MJ, Evrard FL, Jacquerye PG, Picard GR, Lermen OG. Disappearance of essential tremor after stroke. Mov Disord. 2010; 25:2884–2887. [PubMed: 20836089]
13. Erickson-Davis CR, Faust PL, Vonsattel JP, Gupta S, Honig LS, Louis ED. "Hairy baskets" associated with degenerative Purkinje cell changes in essential tremor. J Neuropathol Exp Neurol. 2010; 69:262–271. [PubMed: 20142764]
14. Foscarin S, Gianola S, Carulli D, et al. Overexpression of GAP-43 modifies the distribution of the receptors for myelin-associated growth-inhibitory proteins in injured Purkinje axons. Eur J Neurosci. 2009; 30:1837–1848. [PubMed: 19895561]
15. Foust A, Popovic M, Zecevic D, McCormick DA. Action potentials initiate in the axon initial segment and propagate through axon collaterals reliably in cerebellar Purkinje neurons. J Neurosci. 2010; 30:6891–902. [PubMed: 20484631]
16. Grubb MS, Shu Y, Kuba H, Rasband MN, Wimmer VC, Bender KJ. Short- and long-term plasticity at the axon initial segment. J Neurosci. 2011; 31:16049–16055. [PubMed: 22072655]
17. Harasymiw JW, Bean P. Identification of heavy drinkers by using the early detection of alcohol consumption score. Alcohol Clin Exp Res. 2001; 25:228–235. [PubMed: 11236837]
18. Inoue H, Lin L, Lee X, et al. Inhibition of the leucine-rich repeat protein LINGO-1 enhances survival, structure, and function of dopaminergic neurons in Parkinson's disease models. Proc Natl Acad Sci USA. 2007; 104:14430–14435. [PubMed: 17726113]

19. Kuo SH, Erickson-Davis C, Gillman A, Faust PL, Vonsattel JP, Louis ED. Increased number of heterotopic Purkinje cells in essential tremor. J Neurol Neurosurg Psychiatry. 2011; 82:1038–1040. [PubMed: 20802031]
20. Kuo SH, Faust PL, Vonsattel JP, Ma K, Louis ED. Parallel fiber counts and parallel fiber integrated density are similar in essential tremor cases and controls. Acta Neuropathol. 2011; 121:287–289. [PubMed: 21080179]
21. Llorens F, Gil V, Iraola S, et al. Developmental analysis of Lingo-1/Lern1 protein expression in the mouse brain: interaction of its intracellular domain with Myt1l. Dev Neurobiol. 2008; 68:521–541. [PubMed: 18186492]
22. Llorens F, Gil V, del Rio JA. Emerging functions of myelin-associated proteins during development, neuronal plasticity, and neurodegeneration. FASEB J. 2011; 25:463–475. [PubMed: 21059749]
23. Louis ED, Borden S, Moskowitz CB. Essential tremor centralized brain repository: diagnostic validity and clinical characteristics of a highly selected group of essential tremor cases. Mov Disord. 2005; 20:1361–1365. [PubMed: 16001407]
24. Louis ED, Faust PL, Vonsattel JP, et al. Neuropathological changes in essential tremor: 33 cases compared with 21 controls. Brain. 2007; 130:3297–3307. [PubMed: 18025031]
25. Louis ED, Ferreira JJ. How common is the most common adult movement disorder? Update on the worldwide prevalence of essential tremor. Mov Disord. 2010; 25:534–541. 2010. [PubMed: 20175185]
26. Louis ED, Ma K, Babij R, et al. Neurofilament protein levels: quantitative analysis in essential tremor cerebellar cortex. Neurosci Lett. 2012; 518:49–54. 2012. [PubMed: 22561033]
27. Louis ED, Vonsattel JP, Honig LS, et al. Essential tremor associated with pathologic changes in the cerebellum. Arch Neurol. 2006; 63:1189–1193. [PubMed: 16908751]
28. Luján R, Albasanz JL, Shigemoto R, Juiz JM. Preferential localization of the hyperpolarization-activated cyclic nucleotide-gated cation channel subunit HCN1 in basket cell terminals of the rat cerebellum. Eur J Neurosci. 2005; 21:2073–2082. [PubMed: 15869503]
29. McGee AW, Strittmatter SM. The Nogo-66 receptor: focusing myelin inhibition of axon regeneration. Trends Neurosci. 2003; 26:193–198. [PubMed: 12689770]
30. Mi S, Miller RH, Lee X, et al. LINGO-1 negatively regulates myelination by oligodendrocytes. Nat Neurosci. 2005; 8:745–751. [PubMed: 15895088]
31. Mi S, Miller RH, Tang W, et al. Promotion of central nervous system remyelination by induced differentiation of oligodendrocyte precursor cells. Ann Neurol. 2009; 65:304–315. [PubMed: 19334062]
32. Mi S, Sandrock A, Miller RH. LINGO-1 and its role in CNS repair. Int J Biochem Cell Biol. 2008; 40:1971–1978. [PubMed: 18468478]
33. Mirra SS. The CERAD neuropathology protocol and consensus recommendations for the postmortem diagnosis of Alzheimer's disease: a commentary. Neurobiol Aging. 1997; 18:S91–S94. [PubMed: 9330994]
34. Ogawa Y, Rasband MN. The functional organization and assembly of the axon initial segment. Curr Opin Neurobiol. 2008; 18:307–313. [PubMed: 18801432]
35. Palay, SL.; Palay, VC. Cerebellar Cortex: Cytology and Organization. Springer-Verlag; 1974.
36. Paris-Robidas S, Brochu E, Sintes M, et al. Defective dentate nucleus GABA receptors in essential tremor. Brain. 2012; 135:105–116. [PubMed: 22120148]
37. Satoh J, Tabunoki H, Yamamura T, Arima K, Konno H. TROY and LINGO-1 expression in astrocytes and macrophages/microglia in multiple sclerosis lesions. Neuropathol Appl Neurobiol. 2007; 33:99–107. [PubMed: 17239012]
38. Shao Z, Browning JL, Lee X, et al. TAJ/TROY, an orphan TNF receptor family member, binds Nogo-66 receptor 1 and regulates axonal regeneration. Neuron. 2005; 45:353–359. [PubMed: 15694322]
39. Shill HA, Adler CH, Sabbagh MN, et al. Pathologic findings in prospectively ascertained essential tremor subjects. Neurology. 2008; 70:1452–1455. [PubMed: 18413570]
40. Somogyi P, Hamori J. A quantitative electron microscopic study of the Purkinje cell axon initial segment. Neuroscience. 1976; 1:361–365. [PubMed: 1004711]

41. Sotelo C. Development of"Pinceaux" formations and dendritic translocation of climbing fibers during the acquisition of the balance between glutamatergic and gamma-aminobutyric acidergic inputs in developing Purkinje cells. J Comp Neurol. 2008; 506:240–31. [PubMed: 18022955]

42. Stefansson H, Steinberg S, Petursson H, et al. Variant in the sequence of the LINGO1 gene confers risk of essential tremor. Nat Genet. 2009; 41:277–279. [PubMed: 19182806]

43. Sullivan KL, Hauser RA, Zesiewicz TA. Essential tremor. Epidemiology, diagnosis, and treatment. Neurologist. 2004; 10:250–258. [PubMed: 15335442]

44. Tan EK, Teo YY, Prakash KM, et al. LINGO1 variant increases risk of familial essential tremor. Neurology. 2009; 73:1161–1162. [PubMed: 19805735]

45. Thier S, Lorenz D, Nothnagel M, et al. LINGO1 polymorphisms are associated with essential tremor in Europeans. Mov Disord. 2010; 25:717–723. [PubMed: 20310002]

46. Trojanowski JQ, Revesz T. Neuropathology Working Group on MSA. Proposed neuropathological criteria for the post mortem diagnosis of multiple system atrophy. Neuropathol Appl Neurobiol. 2007; 33:615–620. 2007. [PubMed: 17990994]

47. Vonsattel JP, Del Amaya MP, Keller CE. Twenty-first century brain banking. Processing brains for research: the Columbia University methods. Acta Neuropathol. 2008; 115:509–532. [PubMed: 17985145]

48. Vilarino-Guell C, Ross OA, Wider C, et al. LINGO1 rs9652490 is associated with essential tremor and Parkinson disease. Parkinsoniam Relat Disord. 2010; 16:109–111.

49. Vilarino-Guell C, Wider C, Ross OA, et al. LINGO1 and LINGO2 variants are associated with essential tremor and Parkinson disease. Neurogenetics. 2010; 11:401–408. [PubMed: 20369371]

50. Xie G, Harrison J, Clapcote SJ, et al. A new Kv1.2 channelopathy underlying cerebellar ataxia. J Biol Chem. 2010; 285:32160–32173. [PubMed: 20696761]

51. Yiu G, He Z. Glial inhibition of CNS axon regeneration. Nat Rev Neurosci. 2006; 7:617–627. [PubMed: 16858390]

52. Zonta B, Desmazieres A, Rinaldi A, et al. A critical role for Neurofascin in regulating action potential initiation through maintenance of the axon initial segment. Neuron. 2011; 69:945–956. [PubMed: 21382554]

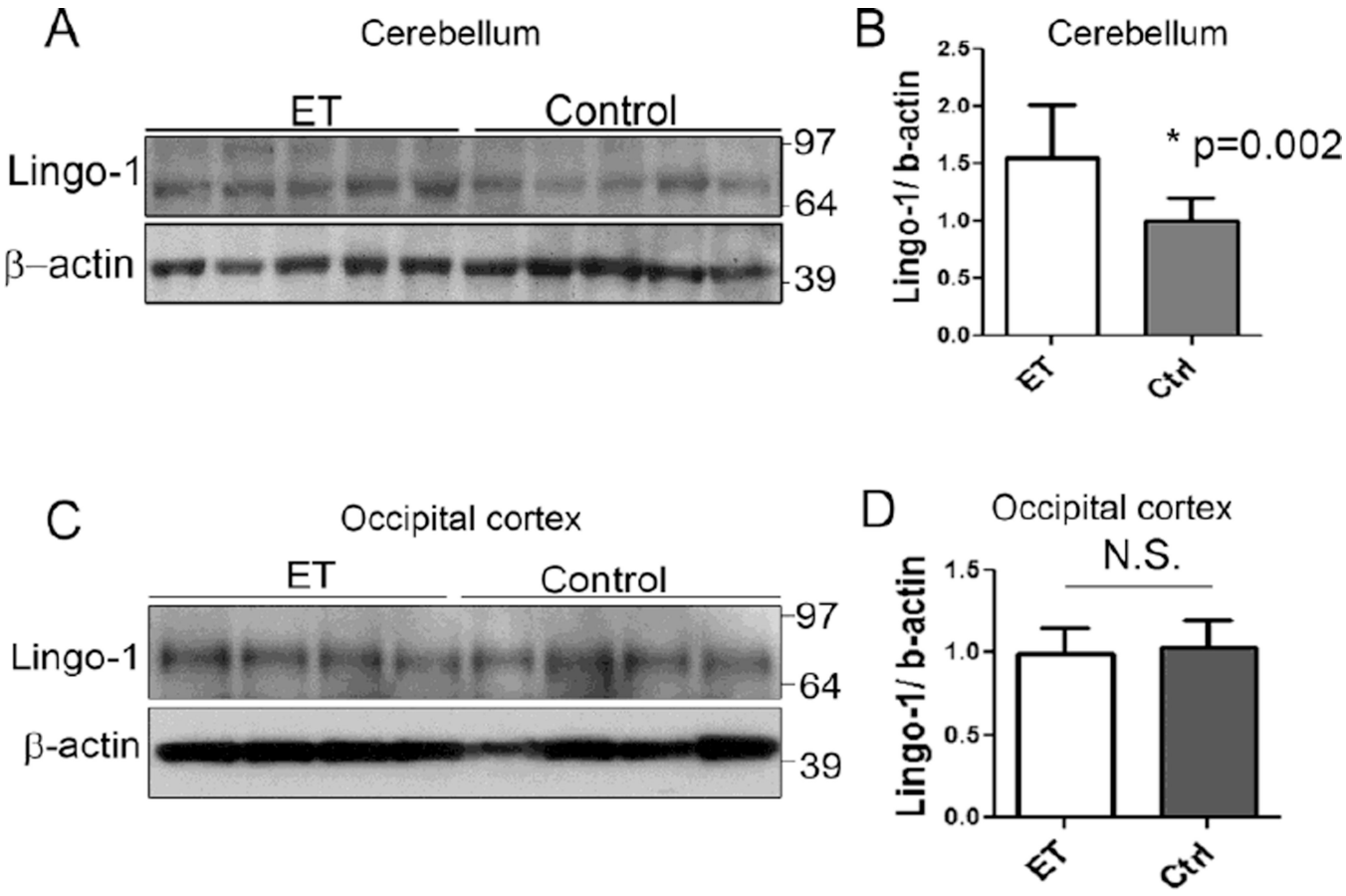

Fig. 1.

Regional increase in Lingo-1 protein level in the essential tremor (ET) cerebellum. Representative Western blots of Lingo-1 from cerebellum (a) and occipital cortex (c) of ET cases and controls. The Lingo-1 protein level, normalized to a β-actin loading control, is significantly increased in ET cerebellum (b) but similar in ET occipital cortex (d), compared to respective control values. The fold-change in Lingo-1 protein level is expressed relative to control brains, which was arbitrarily set at 1.0. Mean ± SD are shown.

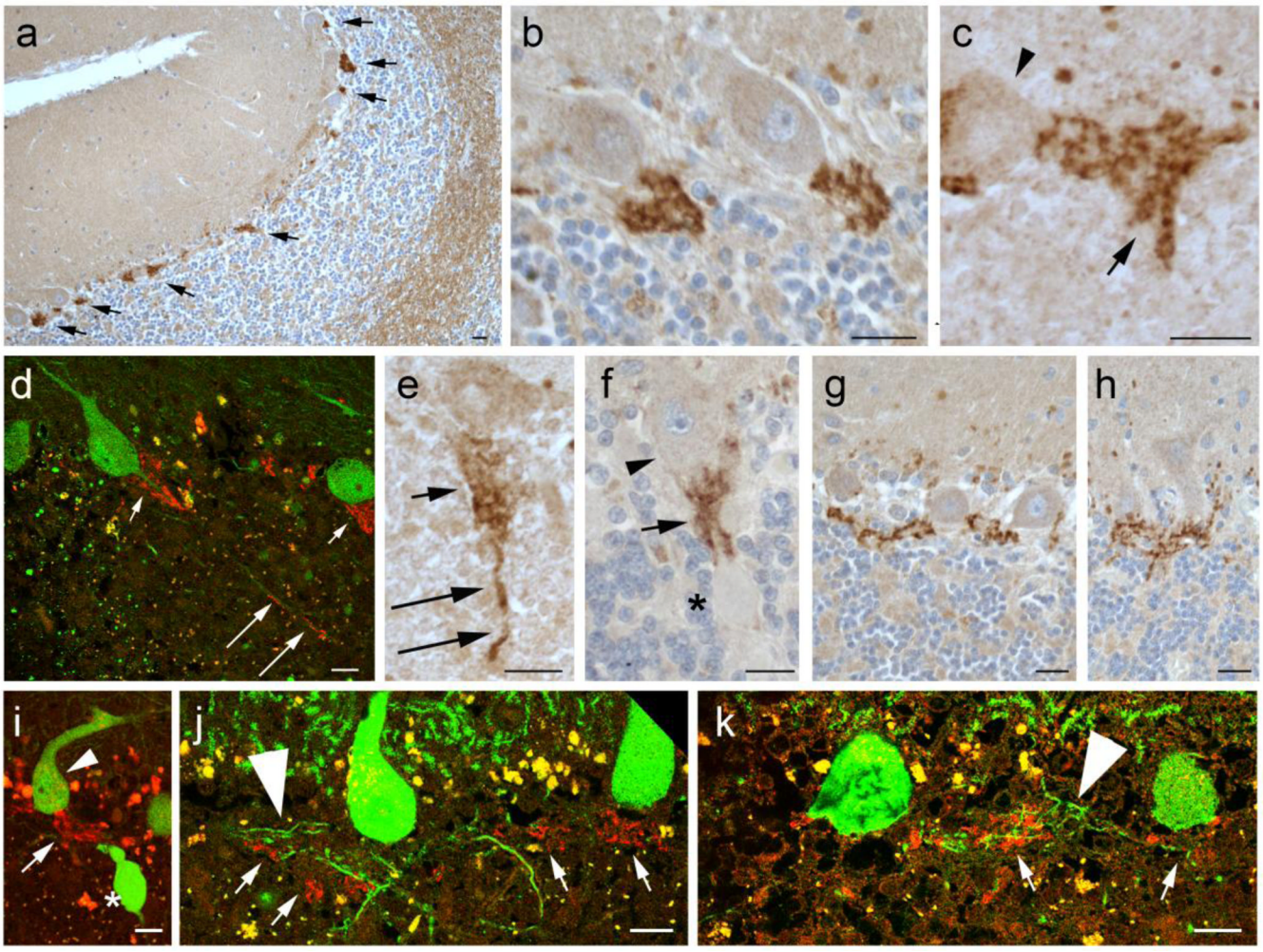

Fig. 2.

Lingo-1 expression in the cerebellar cortex. Immunohistochemistry with Lingo-1 antibody (a–c, e–h) and dual immunofluorescence with anti-Lingo-1 (Alexa 594, red) and anti-calbindinD_{28k} (Alexa 488, green)(d, i–k). Lingo-1 is enriched in a plexus of processes along the PC axon initial segment (AIS) (arrows in a), along with some labeling in white matter along axon profiles and weaker labeling of PC soma and molecular layer (a). The Lingo-1 labeled plexus is often cone-shaped (b–d), and associated with rounded punctate profiles (arrow in c). Lingo-1 labeled processes are occasionally seen along more distal segments of the PC axon (long arrows in d, e). The Lingo-1 labeled plexus surrounds PC axons proximal to axonal torpedoes (asterisk in f, i) and may form complex linear extensions between PC soma (g, h). Lingo-1 labeled plexus may appear in proximity to PC recurrent collaterals (large arrowheads, j,k), but do not consistently colocalize. Small arrowheads: PC bodies; large arrowheads: PC recurrent collateral processes; arrows: Lingo-1 labeled processes; asterisk: torpedo. Scale bar: 20μm.

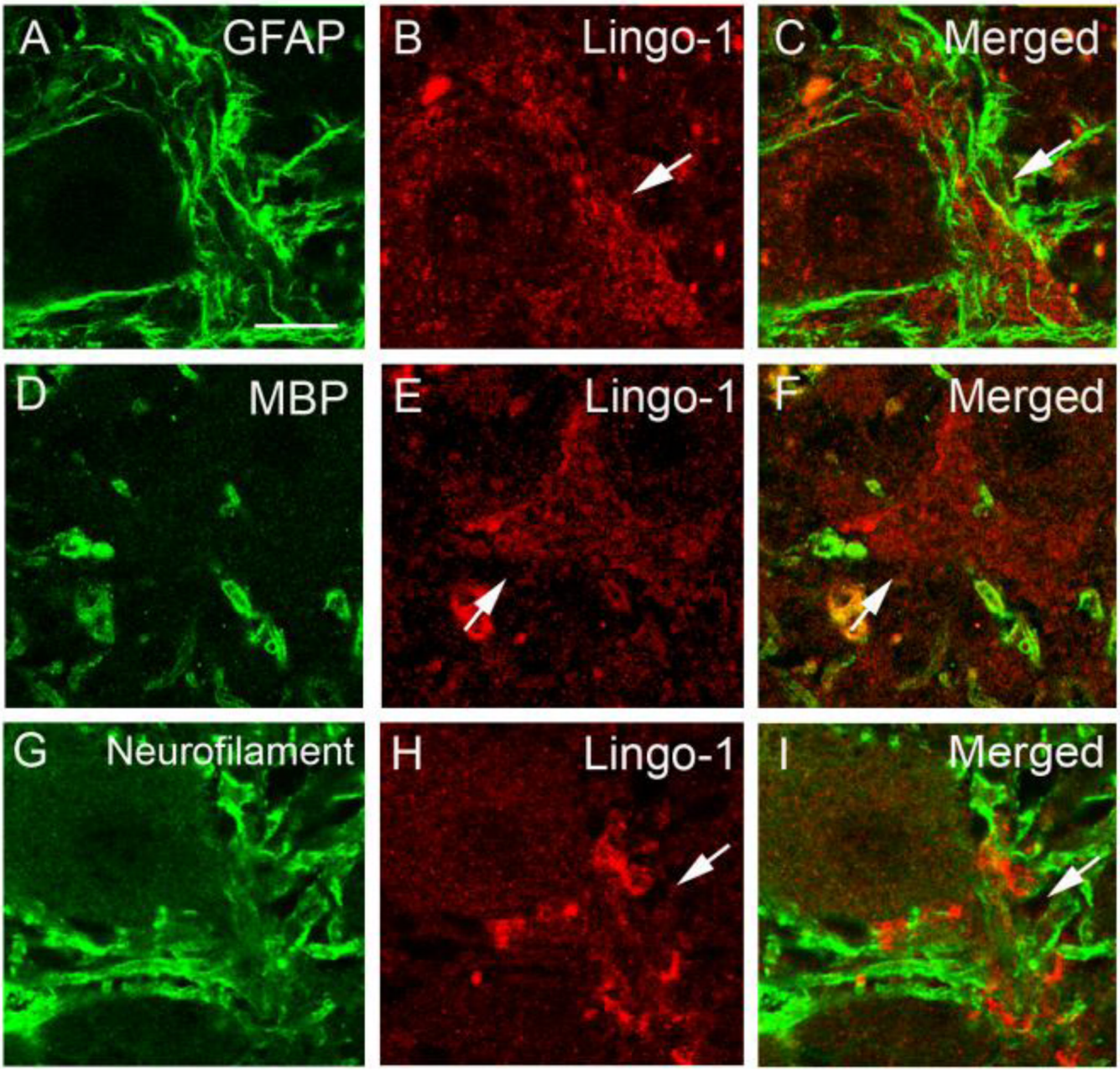

Fig. 3.

Lingo-1 positive plexus did not colocalize with glial markers or neurofilament protein. Dual immunofluorescence labeling of ET cerebellar cortex with anti-GFAP (a), anti-MBP (d), or anti-phosphorylated-neurofilament antibody (g) (Alexa 488, green; a, d, g) and anti-Lingo-1 antibody (b, e, h) (Alexa 594, red). Merged images are shown (c, f, i). Arrow: Lingo-1 positive processes. Scale bar: 25μm

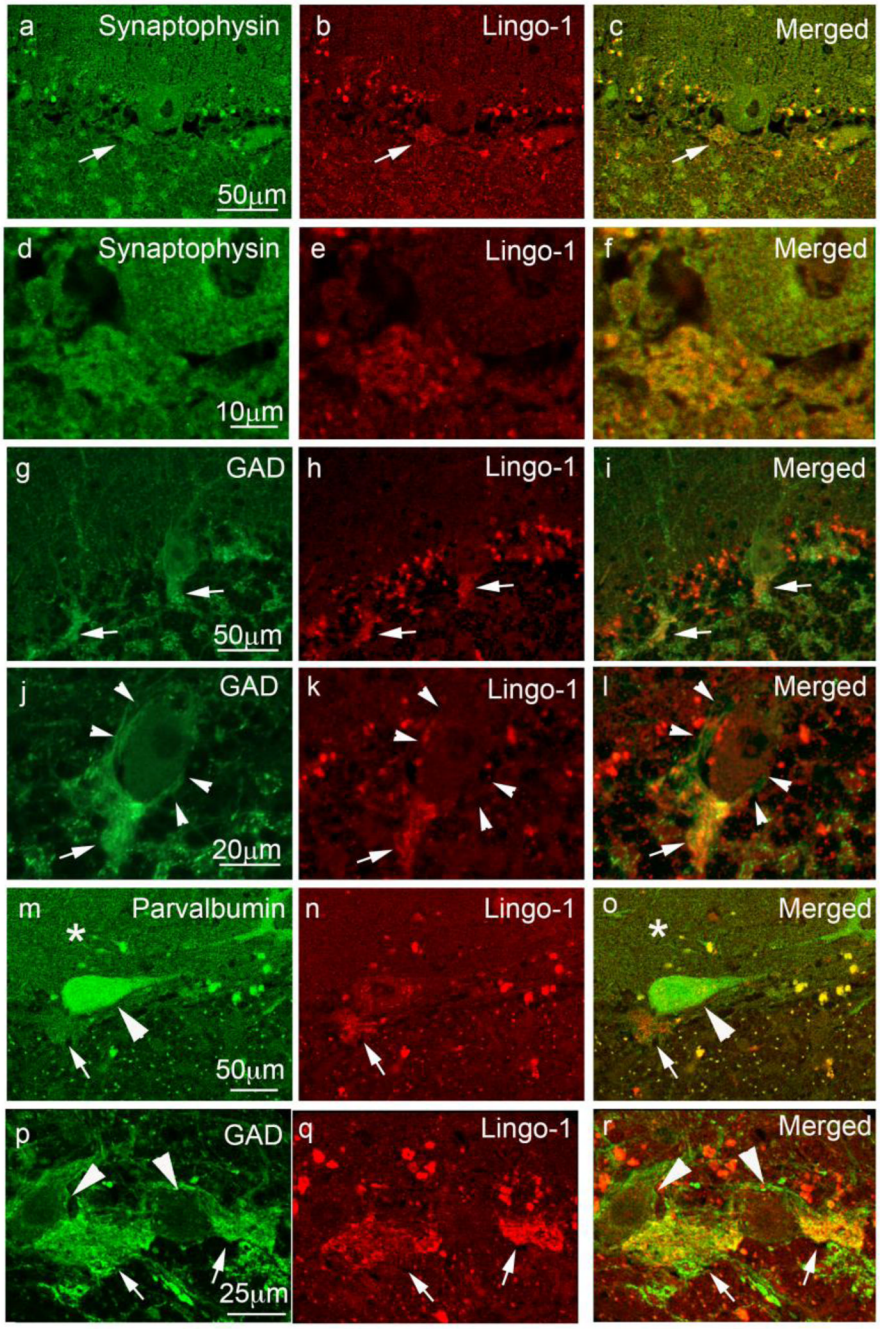

Fig. 4.

Lingo-1 positive fibers colocalize with glutamate decarboxylase (GAD) containing synaptic structures along the PC AIS. Dual immunofluorescence labeling of ET cerebellar cortex with anti-synaptophysin (a, d), anti-GAD (g, j, p), or anti-parvalbumin antibody (m) (Alexa 488, green), and anti-Lingo-1 antibody (b, e, h, k, n, q) (Alexa 594, red). The merged images are shown (c, f, i, l, o, r). Synaptophysin (a–f) and GAD (g–l) colocalized with Lingo-1 positive processes along the PC AIS. GAD-positive fibers surrounding the PC AIS were Lingo-1 positive (arrows in g–l), whereas GAD fibers surrounding PC bodies did not stain for Lingo-1 (arrowheads in j–l). PC bodies (large arrowheads) and PC dendrites in the molecular layer (asterisks) expressed parvalbumin (m, o). Parvalbumin also colocalized with

Lingo-1 positive processes (arrows, m–o). GAD-positive basket cell processes (arrows, p–r) connecting two adjacent PC bodies (large arrowheads, p, r) were also positive for Lingo-1.

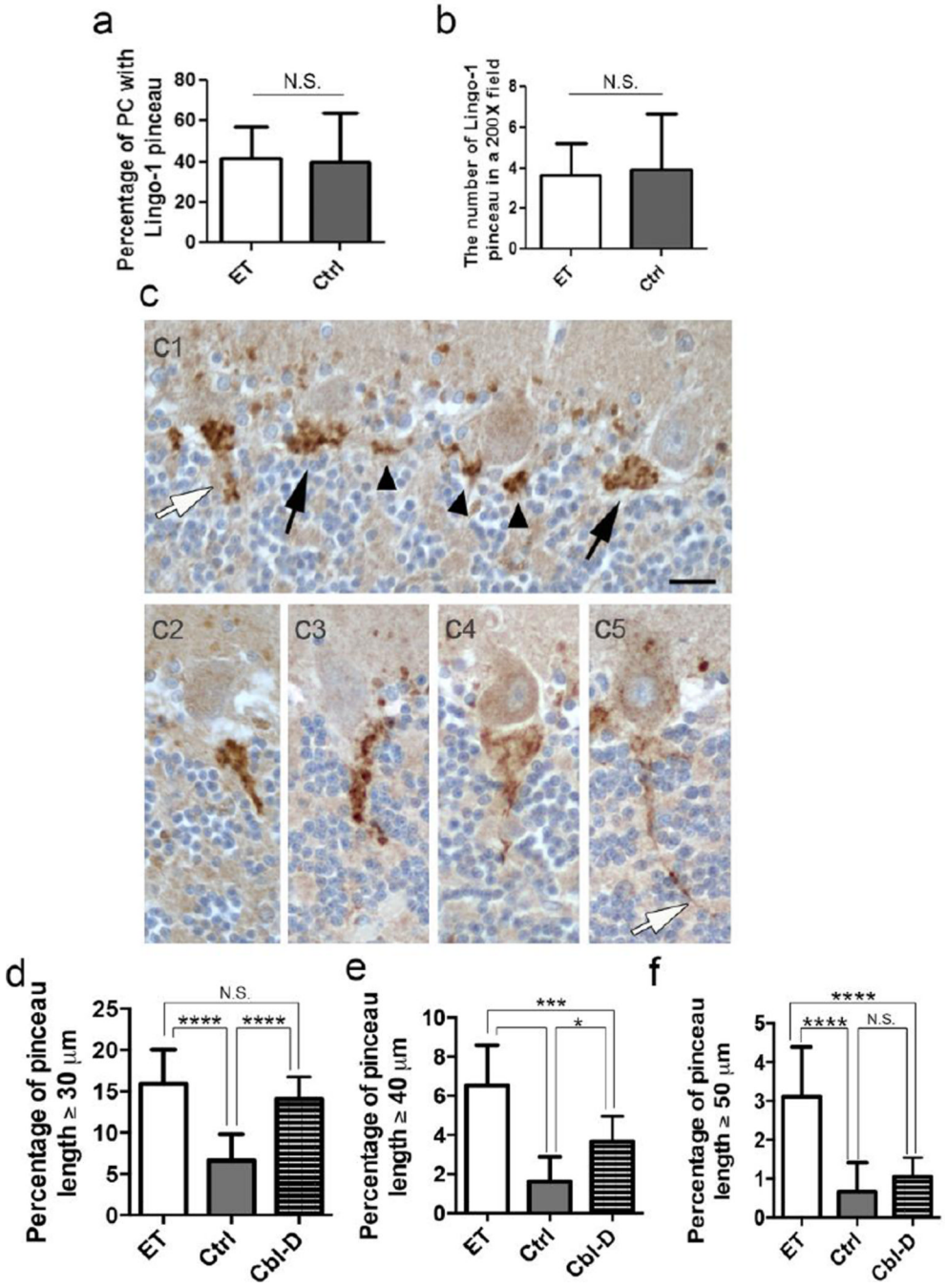

Fig. 5.

Elongated Lingo-1 labeled pinceau processes in ET brains. The percentage of PCs associated with a Lingo-1 positive AIS plexus (a) and the number of Lingo-1 positive plexuses in a randomly selected 200X field (b), was similar in Lingo-1 antibody stained sections of ET cases and controls. Variable appearance of Lingo-1 labeled pinceau in paraffin sections, ranging from very short segments (c1, arrowheads), cone-shaped structure (c1, black arrows), or more elongated forms (c1, white arrow, c2-c5). Lingo-1 labeled pinceau measuring ≥30 μm (d), ≥40 μm (e) or ≥50 μm (f) in length were more frequently seen in ET cases. In comparison with other cerebellar degenerative disorders (Cbl-D), the percentage of Lingo-1 labeled pinceau ≥30 μm was similar in ET cases and Cbl-D cases (d).

However, ET cases had a significantly higher percentage of Lingo-1 labeled pinceau ≥40 μm or ≥50 μm than Cbl-D cases (e,f), and pinceau ≥50 μm are relatively specific to ET (f). *$p \leq 0.05$, ***$p \leq 0.001$, ****$p \leq 0.0001$.

Table 1

Clinical and pathological features of ET cases and controls

	Cerebellar cortex				Occipital cortex	
	Western Blot Analysis		Immunohistochemistry		Western Blot Analysis	
	ET	Controls	ET	Controls	ET	Controls
N	10	11	11	12	7	9
Age at death (years)	85.7 ± 6.1	84.5 ± 6.4	87.3 ± 6.3	83.2 ± 7.5	84.3 ± 8.8	84.8 ± 6.3
Female Gender	5 (50.0%)	6 (54.5%)	9 (81.8%)	8 (66.6%)	3 (42.9%)	5 (55.6%)
Brain Weight (grams)	1211 ± 126	1174 ± 145	1156 ± 126	1222 ± 151	1207 ± 140	1175 ± 157
Postmortem Interval (hours)	3.1 ± 2.3	4.7 ± 2.3	2.4 ± 2.0	8.9 ± 10.5	4.4 ± 3.8	4.1 ± 1.7
Braak AD Stage	2.0 ± 1.2	2.0 ± 1.1	2.6 ± 1.3	1.7 ± 0.6	1.6 ± 1.0	2.0 ± 1.1
CERAD Plaque Score						
0	5 (50.0%)	5 (45.5%)	5 (45.4%)	7 (58.3%)	4 (57.1%)	5 (55.6%)
A	3 (30.0%)	3 (27.3%)	3 (27.3%)	3 (25.0%)	1 (14.2%)	1 (11.1%)
B	2 (20.0%)	3 (27.3%)	2 (18.2%)	2 (16.6%)	2 (28.6%)	3 (33.3%)
C	0 (0.0%)	0 (0.0%)	1 (9.0%)	0 (0.0%)	0 (0.0%)	0 (0.0%)
Lewy Body Pathology	ILB, 2 (20%)	None	None	None	None	None
Basket plexus rating	2.0 ± 0.9	1.8 ± 0.4	2.2 ± 0.9	1.6 ± 0.6	2.0 ± 0.9	1.9 ± 0.7
Axonal Torpedoes *	11.1 ± 8.5	3.4 ± 2.7	11.0 ± 8.1	2.2 ± 1.3	14.9 ± 1.4	2.6 ± 1.4

ILB: very rare, incidental Lewy bodies, in brainstem nuclei only;

* $p<0.05$